Research Article

Finite Element Analysis of Fluid Flow through the Screen Embedded between Parallel Plates with High Reynolds Numbers

Abid A. Memon,[1] **Hammad Alotaibi,**[2] **M. Asif Memon** ⓘ**,**[1] **Kaleemullah Bhatti,**[1]
Gul M. Shaikh,[1] **Ilyas Khan** ⓘ**,**[3] **and A. A. Mousa** ⓘ[2]

[1]*Department of Mathematics, Sukkur IBA University, Sindh, Pakistan*
[2]*Department of Mathematics and Statistics, Faculty of Science, Taif University, P.O.Box 11099, Taif 21944, Saudi Arabia*
[3]*Faculty of Mathematics and Statistics, Ton Duc Thang University, Ho Chi Minh City 72915, Vietnam*

Correspondence should be addressed to Ilyas Khan; ilyaskhan@tdtu.edu.vn

This paper provides numerical estimation of Newtonian fluid flow past through rectangular channel fixed with screen movable from 10° to 45° by increasing the Reynolds number from 1000 to 10,000. The two-dimensional incompressible Navier Stokes equations are worked out making use of the popular software COMSOL MultiPhysics version 5.4 which implements the Galerkin's least square scheme to discretize the governing set of equations into algebraic form. In addition, the screen boundary condition with resistance coefficient (2.2) along with resistance coefficient 0.78 is implemented along with slip boundary conditions applied on the wall. We engaged to find and observe the relationship between the optimum velocity, drag force applied by the screen, and pressure occurred in the channel with increasing Reynolds number. Because of the linear relationship between the optimum velocities and the Reynolds number, applying the linear regression method, we will estimate the linear equation so that future prediction and judgment can be done. The validity of results is doing with the asymptomatic solution for stream-wise velocity at the outlet of the channel with screens available in the literature. A nondimensional quantity, i.e., ratio from local to global Reynolds number Re_x/Re, is introduced which found stable and varies from -0.5 to 0.5 for the whole problem. Thus, we are in the position to express the general pattern of the velocity of the particles as well as the pressure on the line passing through the middle of the channel and depart some final conclusion at the end.

1. Introduction

The screens are commonly used in the gauze machines of the air crafts and electronic elements like air conditions, air cooler, and fans, to transmit the air or turning down the heat into the medium by speeding the fluid flow. For supervisory, the speed, pressure, and drag forces once the fluid of any type turns up into the area are the foremost problem in the field of engineering sciences. For the resolution and to overwhelm the enigma of the problem, the screens have been recycled for the decades. A solid screen or any type of the screen has the competency to turn or subdue the tangential component of the velocity field to enhance a little speed of the fluid. Although any metallic screen included the channel, the angle of inclination at which the screen is put into the channel bears the matter. The angle will become convenient for the

purpose where we want to optimize one of the parameter from velocity magnitude, pressure, drag force, etc. In order to develop the perfect design for an engineering tool, it is the best to perceive the flow distribution among the channels with screens. This problem will help the researchers or scientists to understand the mechanism of optimized velocity and pressure connected with Reynolds number while performing the experiment of flow through the screens and also a general pattern of the velocity of the particles and the pressure with respect to the local to global ratio of the Reynolds numbers.

Numerous scientists and engineers laid their trials in order to comprehend the fluid flow phenomenon observed when the screens are ascribed in the channel. The Elder [1], in 1959, discovered the asymptotic solution for the small angle of inclination of the screen by testing the fluid flow via the channel consists of the single screen. Several

experiments were conducted by Wang and Santiago [2] to detect the head loss/energy loss while the fluid moves with screen added at some angles. They came up with that the head loss or energy loss alters to slower as reducing the angles of the screens. Abid et al. [3] applied the Galerkin's least square scheme of finite element method and to perform on the whole procedure by commercial software COMSOL MultiPhysics 5.4 discussed the fluid flow thorough the three screens arranged -45° to 45° judged from the center of the screens at the equal distance from each other. He uncovered that adding more screens will speedy the fluid flow and relationship between the optimized velocity with the angle and optimized pressure with the angle of inclination of the screen that can be shaped. To comprehend the fluid flow phenomenon of the rough particles when a vibrating screen attached in the angle, Sawant et al. [4] used Discrete Element Method. He recommended that by improving the angles of the screen, the maximum mass of the rough particles is achievable to cross through the screen. Using the different values of porosities (0.4, 0.52, and 0.6) and attached the screens at 450 and 1500 performed the lab experiment and applying the same model in the ANSYS CFX-II software package, the fluid flow phenomenon is developed and checked by Teital [5]. He discovered that mass flow rate is maximum across the screen when the screens are attached either at 45° or at 135°. Hauke and Hughes [6] presented the new formulation known as Galerkin's least square scheme (GLS) to get Navier Stokes equation solved numerically for compressible flows and can be applied for any set of variables. It was found that if the entropy or primitive variables are chosen like pressure, velocity field, and temperature, then the formulation will be working well for incompressible flows also. Therefore, one formulation can be used to solve both compressible and incompressible flows. A numerical and statistical analysis [7] was done to enhance the understanding of the relationship between maximum velocity as well as pressure. For the purpose, an air flow through the three screens with different inlet velocities was tested with different resistance coefficients. It was found that with the increase in inlet velocity, the relationship between the maximum velocity at the outlet and resistance coefficient weakens whereas optimum pressure always shows the strong compatibility with the resistance coefficient. A laminar and Newtonian fluid flow was observed [8] for measuring reattachment length as well as velocity patterns in the backward step channel with the boost of FEM technique and carrying the process on COMSOL MULTIPHYSICS 5.0 for the simulation. It was proved with the simulation that the length of reattachment showed a good agreement with the data available in the literature, and the simulation contributed full understanding of the velocity pattern in the domain. A Couette flow was observed by solving the equations of the second grade fluid with the extension of the shift of variables with the slip and no-slip boundary conditions on the walls [9]. It was seen that due to the application of slip conditions, very less fluctuations were appearing in the case of velocity field along the wall and that observation was quite different in the case of no-slip condition. To generate the time dependent pressure gradient with the trapezoidal rule, a little effort of Fourier series along with

the implementation of oscillation of Burger's equation was taken to investigate a circular tube with the porous medium [10]. It was sought that for all sources of Burger's equation, the forces at the wall surface are declining because of increasing the porosity level in the tube. A most effective Thomas algorithm of finite difference method was applied over the nondimensional Navier Stokes equation to investigate the funnel flow along with the micropolar fluidic medium [11]. The investigation determined the velocity distribution along with the pressure distribution for the both behaviours of microfluidic as well as funnel flows. By adding some physical terms in the differential equations of higher order, the study through the investigation was conducted for the two types of oscillatory flows (Kamenev-type and Philos-type) and the asymptotic characteristics in the two articles [12, 13]. The characteristics explained in the articles were proven with the benchmark examples. Moreover, with the implication of least square Galerkin's scheme via the COMSOL MultiPhysics 5.4, the shear thinning as well as shear thickening fluid through the three screens was discussed with the effect of high Reynolds number [14]. Excellent achievements were done as the empirical linear and quadratic equations in account of Reynolds number for the optimum velocity and as well as for the pressure were deducted for the future predictions for such flows. With the use of hybrid nanofluid (a well-known coolant), a heat transfer procedure in a heat exchanger of industrial length containing the double tube with presence of magnetic field on it, a numerical study [15] was carried out. The heat transfer performance was checked with the volume fraction from 0.1% to 0.5% and the Reynolds numbers 800-2400 for the two hybrid nanofluids $CNT-Al_2O_3$ and $CNT-Fe_3O_4$. It was found that the heat transfer performance of the hybrid nanofluid $CNT-Fe_3O_4$ on the basis that the Nusselt number is enhancing in the presence of magnetic field. With the procedure of similarity method [16], the governing nonlinear partial differential equations were converted in to ODEs to check the influence of the radiation for the CCHF model along with the entropy generation in terms of the prominent constants. The results were discussed for several parameters like temperature, entropy, and concentration, and it was specially discussed that the entropy is increasing with the Biot number, Hartman number, and suction as well as injection, constants, etc.

The objective of my study is to analyze the fluid flow through the single screen fitted in the rectangular channel. The fluid is assumed Newtonian, laminar, and steady state. And the whole numerical results are attained by applying the Galerkin's least square scheme of finite element method, and the whole process is carrying on COMSOL MultiPhysics 5.4. The pattern of fluid is to be examined by using the Reynolds number from 1000 to 10,000 and obtained the empirical equations for optimized speed and pressure in the domain for the angles 100 to 450. The outcomes are presented through surface plots for the velocity field and pressure. Additionally, the calculations of the drag force applied by the screen and the velocity as well as the pressure on the average line at the middle of the channel have expressed in terms of the ratio from local to global Reynolds numbers are presented with graphs. Trustworthy results are
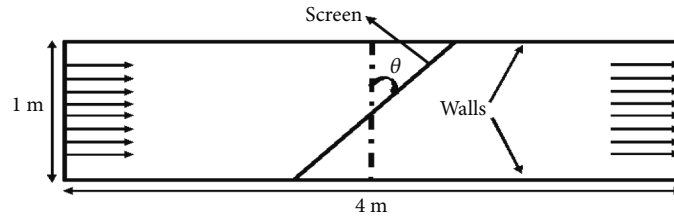
FIGURE 1: Geometrical construction of the channel.

TABLE 1: Mesh statistics.

Property name	Value
Minimum quality element	0.7629
Maximum quality element	0.9793
Number of triangular elements	2382
Edge elements	215
Vertex elements	10

achieved as we compare and contrast the result with available literature.

2. Methodology

2.1. Geometrical Structure and Meshing Process. The two-dimensional rectangular channel with the dimension 4×1 in length to width is taken, see Figure 1. A solid screen is placed at the center of the channel which is portable from $10°$ to $45°$ in clockwise direction. The left wall of the channel is taken up entrance of the fluid with an average velocity of u_{in}. The right wall of the channel is facing the outlet boundary condition and zero pressure. The upper and lower boundaries of the channel are fixed, and slip boundary conditions are applied. The problem is being combated by using the software COMSOL MultiPhysics 5.4 which implemented the numerical method of Galerkin's scheme of least square. Every numerical method basic requirement is to decompose the whole domain into smaller domains called elements. Here, the channel is decomposed in 2382 irregular triangular elements. The whole mesh statistics is described by Table 1 and the meshing of the geometry by Figure 2.

2.2. Governing Equations. It has been decades that the Navier Stokes equations assist to apprehend the physical problems of fluid dynamics. Owing to the nonlinearity of the set of partial differential equations, it is almost incredible to acquire the preferred function (implicit or explicit) without considering the some assumptions which is not but an agreement or dealing with the solution. In the problem, we searched to understand the flow phenomenon through the single screen using the new technique of Galerkin's least square finite element method [6] carrying in the emerging software COMSOL MultiPhysics 5.4. The problem is two-dimensional, steady state, laminar, incompressible, and Newtonian. We will acquire the numerical solution by solving the two-dimensional incompressible Navier Stokes equation, i.e., momentum equation along with the continuity equation

with the screen boundary condition, where the screen is attached at the middle of the geometry with an angle measured clockwise from the center of the screen. The 2nd order partial momentum equation and continuity equation are described below.

$$\frac{\partial \vec{V}}{\partial t} + \left(\vec{V}.\nabla\right)\vec{V} = -\frac{1}{\rho}\nabla p + \mu\nabla^2\vec{V} + F, \tag{1}$$

$$\nabla.\vec{V} = 0, \tag{2}$$

$$\frac{\partial \vec{V}}{\partial t} = 0, \tag{3}$$

where μ and ρ are the viscosity and density of the air. Equations (1) and (2) are called Navier Stokes equations and are in vector form, where $\vec{V}$, p, and F are the velocity field, pressure, and forcing function. Because the chosen problem is steady state that is why we will have equation (3). In the selected geometry, the upper and lower boundaries are considering the wall and slip boundary conditions that are applied on it. Why is the slip boundary condition? The viscous effect near the wall is assumed zero here. If $\vec{n}$ is the vector normal to the velocity field then:

$$\vec{V}.\vec{n} = 0,$$
$$\vec{K} - \left(\vec{K} - \vec{n}\right)\vec{n} = 0, \tag{4}$$

where

$$\vec{K} = \nu\left(\nabla.\vec{V} + \left(\nabla.\vec{V}\right)^T\right)\vec{n}. \tag{5}$$

The working fluid comes into the entrance of the channel passing across the screen and goes out from the outlet of the channel. The screens are actually a solid too to increase the speed of the fluid which suppresses the tangential component of the vector velocity to boost the speed in the channel of the fluid. We define the screen boundary condition by the equations (6)–(8):
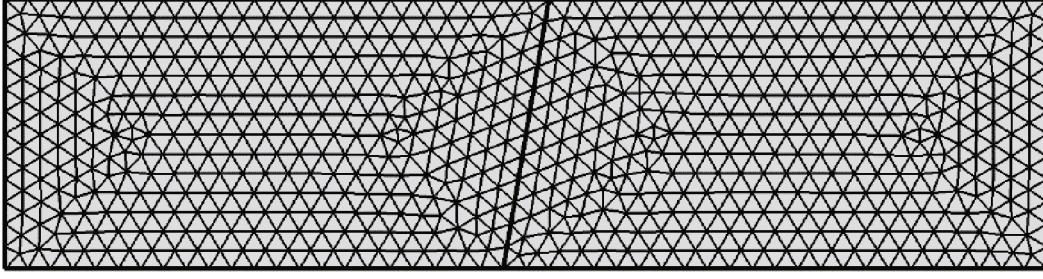
$$\left[\rho\vec{V} - \vec{n}\right]_-^+ = 0, \tag{6}$$

FIGURE 2: The meshing of the geometry with irregular triangular elements.

$$\left[\rho - \left(\overrightarrow{n}\right)^T K \overrightarrow{n} + \rho \left(\overrightarrow{V} \times \overrightarrow{n}\right)^2\right]_-^+ = -\frac{K}{2}\rho - \left(\overrightarrow{V}- \times \overrightarrow{n}\right)^2, \tag{7}$$

$$\overrightarrow{n} \times \overrightarrow{V_+} = \eta \left(\overrightarrow{n} \times \overrightarrow{V_-}\right). \tag{8}$$

In equations, "+" and "−" show the presents of the parameter up and downstream, respectively. To test the fluid flow phenomenon, it is the traditional to use of nondimensional Reynolds number (Re). On applying the inlet boundary condition, the fluid is allowed to enter with the average velocity μ_{in}. Let L be the characteristic length of the channel, then we can define the Reynolds number:

$$R_e = \frac{\rho \mu_{in} L}{\mu}. \tag{9}$$

2.3. Validation and Comparison. The similar geometry is contemplated by Elder [1] and discovered the asymptomatic solution given by equation (10):

$$\frac{(\mu/\mu_{in} - 1)(1 + \eta + k \cos^2\theta)}{(1 - \eta)\tan\theta\, k\, \cos^2\theta} = \frac{2}{\pi}\log\left(\cot\left(\frac{\pi y}{2}\right)\right), \tag{10}$$

where μ is the fluid velocity magnitude computed numerically. Left hand side of the equation presents the stream-wise velocity computed numerically, and right hand side is independent of the numerical calculations but having the same meaning as left hand side. In this spot, we calculate the stream-wise velocity at the outlet of the channel at $R_e = 10,000$ with angles of 10°, 20°, 30°, 40°, and 45°. Figure 3 shows that the approach contributes good alliance to recognize the fluid flow through solid screens employing the finite element approach with Galerkin's least square procedure.

2.4. Result Discussion. We have gained the numerical outcomes using the least square Galerkin's approach of finite element techniques using the commercial software COMSOL MultiPhysics 5.4 by fixing resistance coefficient k at 2.2 and refraction coefficient η at 0.78.

The results are attained and passed through the validation and resemblance process with that asymptomatic solution provided by equation (10). The surface plot for the velocity field and distribution of the pressure is demonstrated
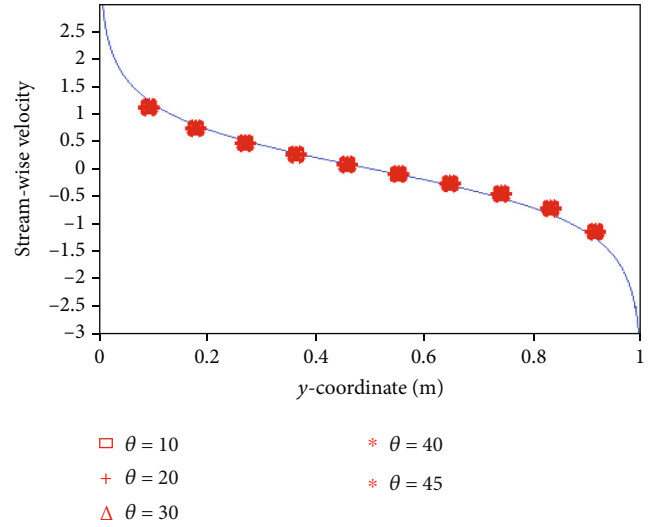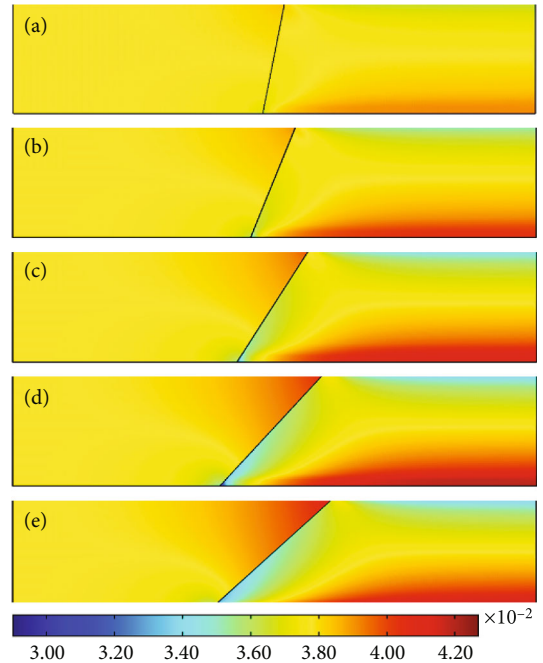

□ $\theta = 10$	* $\theta = 40$
+ $\theta = 20$	* $\theta = 45$
△ $\theta = 30$	

FIGURE 3: Comparison by equation (10).

FIGURE 4: The surface plot of the velocity field at angles 10°-45° from (a–e).
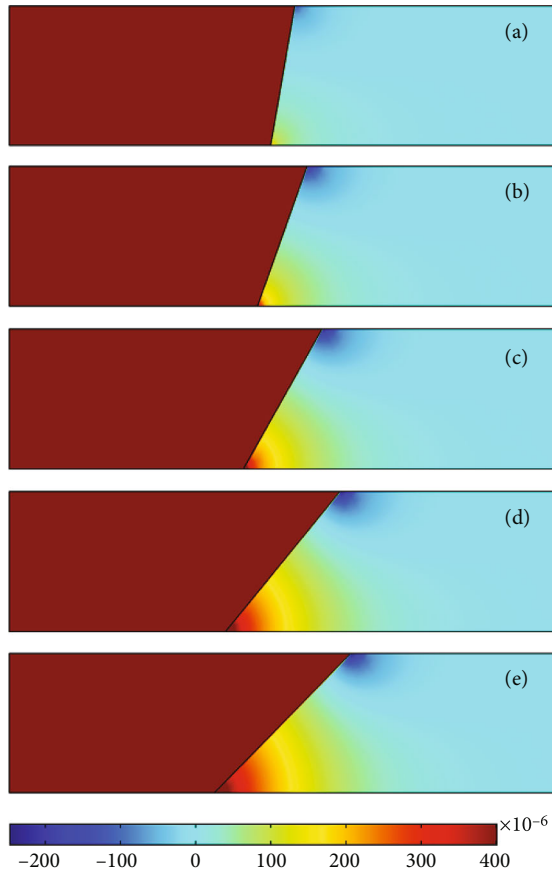
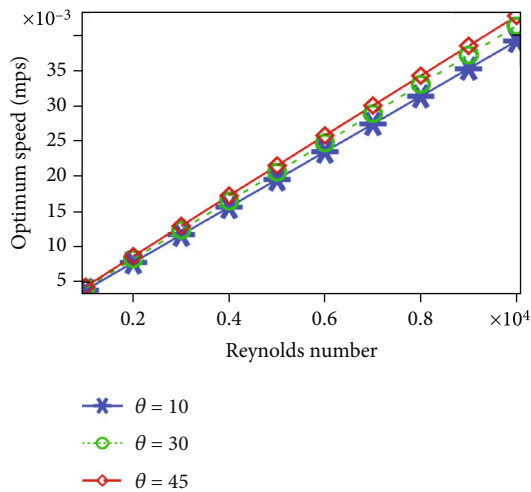FIGURE 5: The surface plot of the pressure distribution at angles 10°-45° from (a–e).

FIGURE 6: The optimum speed is the linear function of the Reynolds number.

TABLE 2: Linear regression equations.

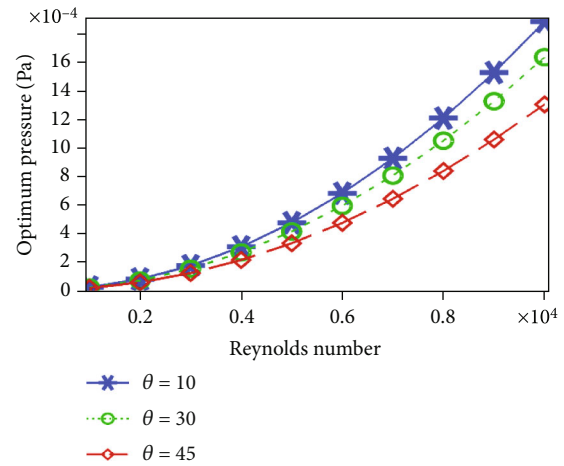| Angles	Equations Domain: $1000 < Re < 10,0000$
10°	$V_{\max} = (3.916E - 6)R_e - 3E^{-5}$
20°	$V_{\max} = (4.043E - 6)R_e - 5E^{-5}$
30°	$V_{\max} = (4.121E - 6)R_e + 3E^{-5}$
40°	$V_{\max} = (4.182E - 6)R_e + 18E^{-5}$
45°	$V_{\max} = (4.253E - 6)R_e + 2E^{-4}$

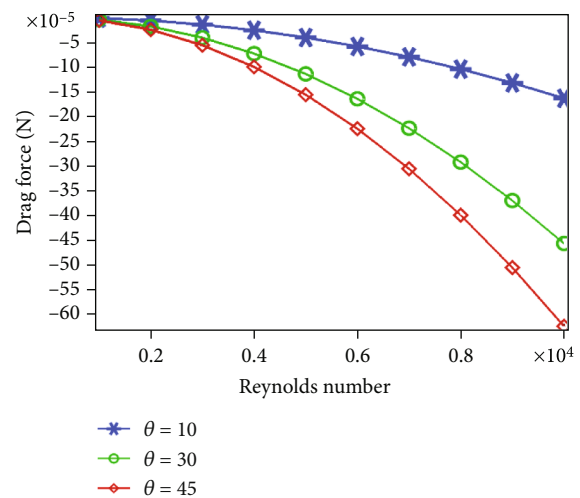FIGURE 7: The optimum pressure is the function of Reynolds number.

FIGURE 8: The drag force (N) is calculated at the screen for all Reynolds number with the angles 10°, 30°, and 45°.

through Figures 4 and 5 at Reynolds number 10000. From Figure 4, it is evident that whatever the screen is arranged at the angles from 10° to 45°, the speed of fluid is increasing. Significantly, it is to be perceived that distribution of the speed of fluid particles is not consistent after the screen as we can see the portion near down the outlet, where the fluid

has maximum speed. This is because of the angle of the screen which is settled at 10° to 45° which push or forcing the fluid in downward direction.

Figure 5 shows the distribution of the pressure in the domain. It can be spotted that screens are culpable to ease pressure in the domain. Furthermore, the results demonstrate that ahead of the screen, the pressure distribution is consistent, and while after the screen, the pressure
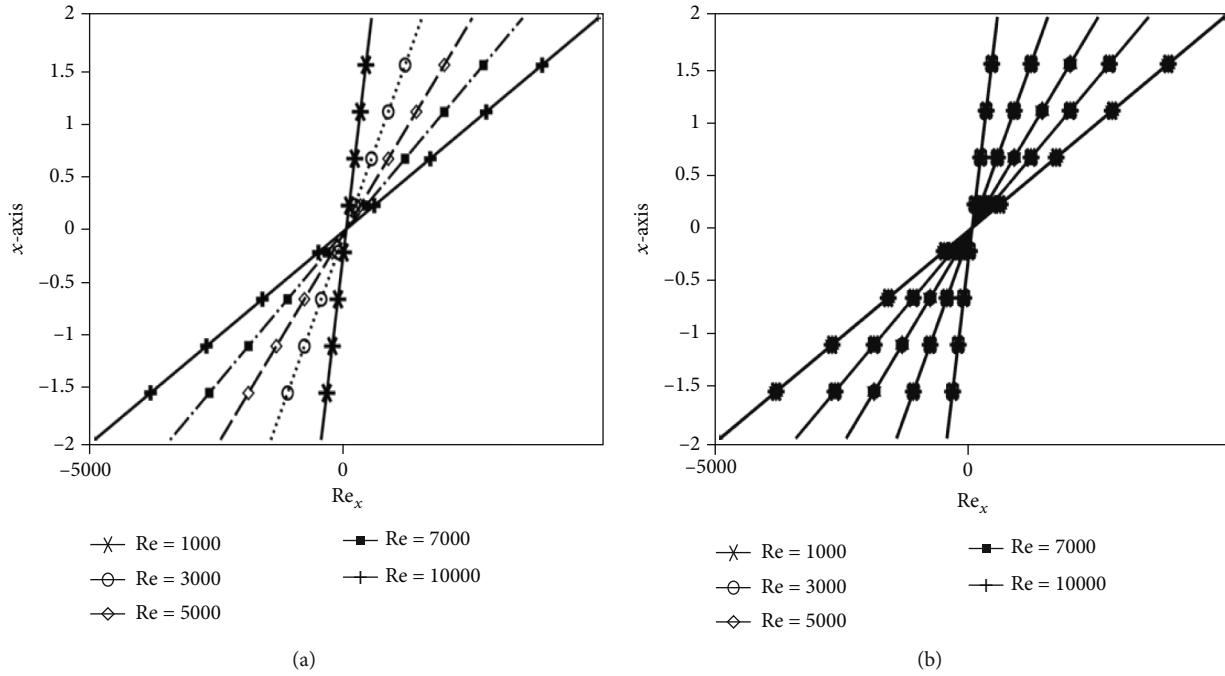
(a)

(b)

Figure 9: (a) The local Reynolds number (Re_x) vs. the x-axis for the angle 45° and (b) the local Reynolds number (Re_x) for all angles 10°-45°.
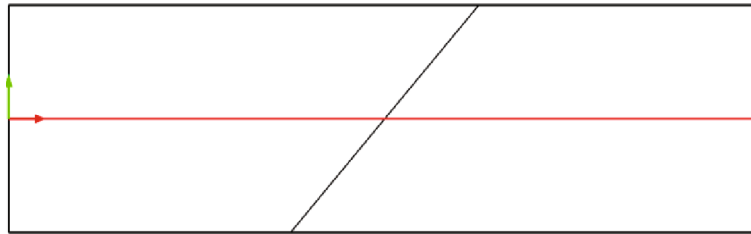

Figure 10: The view of the line at the middle of the channel.

distribution is not uniform as minimum pressure can be spotted on the upper corner of the screen. When the screen is rushed from 10° to 45°, the optimum velocity of the fluid evidences the greatest response in terms of increment in speed of the fluid for all Reynolds number, see Figure 6.

The optimum speed of the fluid is increasing in linear fashion with the increase in Reynolds number for all angles. Figure 6 describes the influence of the optimum speed of the fluid taking place in the domain in terms of Reynolds number. In this way, using the data points and putting in the linear regression procedure, a linear relationship between the optimum speeds with that of nondimensional number can be determined for each angle known as empirical equations, see Table 2.

We have also worked out of the results for optimum pressure existed at each Reynolds number for each angle.

Figure 7 indicates that optimum pressure does not possess a linear but a quadratic relationship. Of course, optimum pressure is increasing with the increase in Reynolds number, and also due to changing the screen from 10° to 45°, the opti-
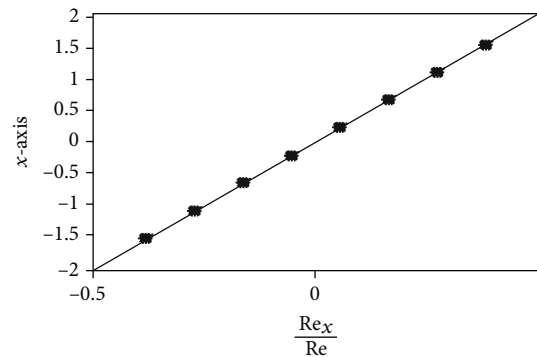

Figure 11: The ratio local to global Reynolds number for all the angles.

mum pressure is dropping for all Reynolds number. Engineers are often attracted for the design analysis, and to design any equipment, they are most charming towards controlling the drag force applied on the domain. The drag force
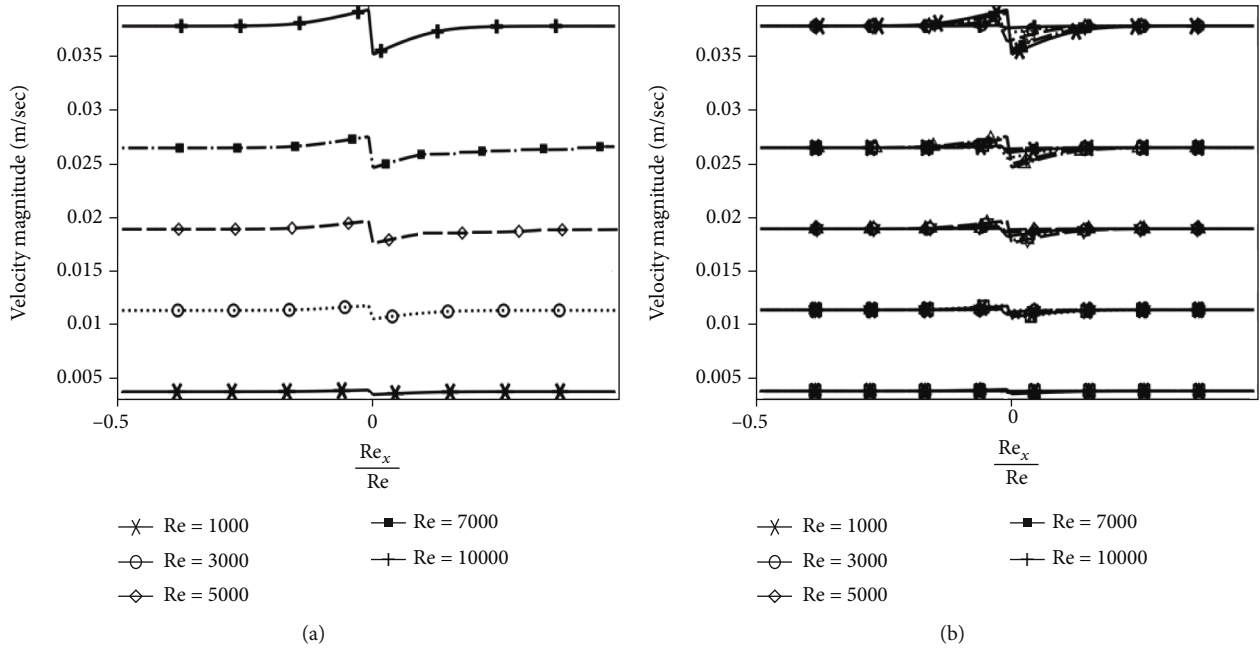
(a)

(b)

FIGURE 12: (a) Re$_x$/Re vs. the x-axis at angle 45 at the Reynolds number; (b) Re$_x$/Re for all the angles at the Reynolds number.
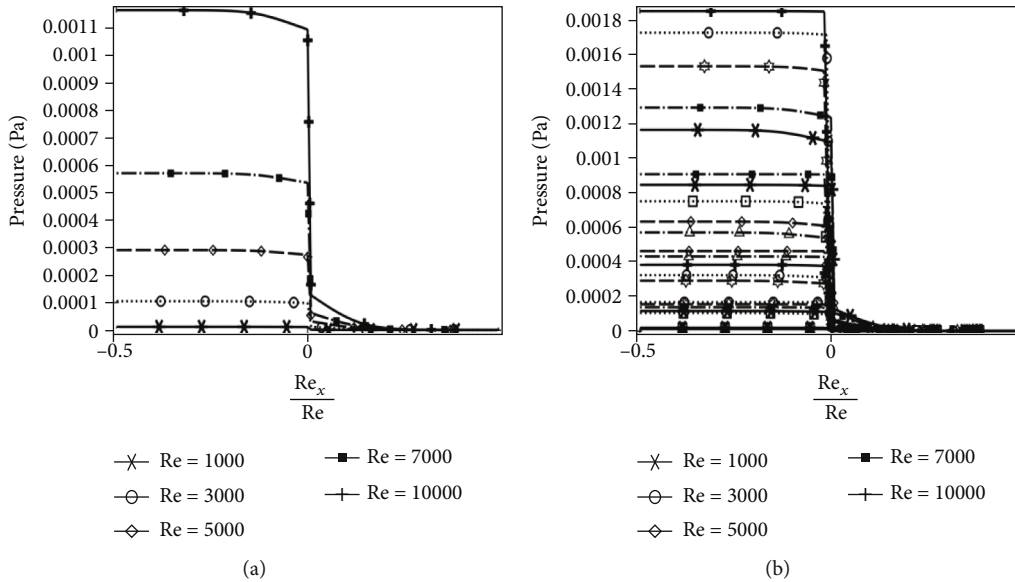

(a)

(b)

FIGURE 13: (a) Re$_x$/Re vs. the x-axis at angle 45 at the Reynolds number; (b) Re$_x$/Re for all the angles at the Reynolds number.

can be controlled by equation (11):

$$F_d = \frac{1}{2}\rho v^2 C_d A, \tag{11}$$

where F_d is the drag force on the screen, C_d is the nondimensional area of the channel, A is the cross-sectional area of the channel, and v is the velocity of the fluid.

The drag force is indeed the measure of the resistance force while the fluid facing in a precise direction. Yet, there have been several approaches to determine to the drag force in different ways. In COMSOL MultiPhysics 5.4, we determine the drag force on the single screen by integrating the total stress in y-direction. The outcomes calculated are disseminated through Figure 8, and it is clear that turning the screen from 10° to 45°, the drag force is decreasing with the boost in Reynolds number.

In the paper, we have added the special description for the local Reynolds number that can be defined by the equation.

$$\text{Re}_x = \frac{\rho u_{\text{in}} x}{\mu}. \tag{12}$$

The local Reynolds number is calculated (shown in Figures 9(a) and 9(b)) for the all Reynolds number along

the line at the middle of the channel as shown in Figure 10. In Figure 9(a), at 45°, it can be seen that the value of the local Reynolds number is linearly increasing even at the middle of the channel where we have seen that the screen will show full impact of it. In Figure 10(b), that impact shows the constancy even for all the angles for corresponding Reynolds numbers. The ratio from local Reynolds number to global Reynolds number shows the stability and attempts the range $-0.5 \leq \mathrm{Re}_x/\mathrm{Re} \leq 0.5$ for all the angles of the screen, see Figure 11. So we find the best to describe the velocity and the pressure on the average path of the channel described by Figure 10, in terms of the ratio from global to local Reynolds numbers. It is observing that the orientation of the fluid passing through the screen is disturbed by the screen for the velocity field as well as in the pressure, see Figures 12(a), 12(b), 13(a), and 13(b). For the velocity field, once the fluid particles disturbed then recover the actual flow rate in the domain after the screen. While observing the pressure of the fluid in the domain once the pressure is reduced then remains constant after the screen. Therefore, we can say that the screens are pressure reducing tools. The problem described the pattern for the movement of flow in the porous media which is so complicated to organize for the single layer of the porous path. On the whole, it can be deducted that the greater the Reynolds number, the greater the velocity and the greater the disturbance occur.

3. Conclusion

The two-dimensional flow past the rectangular channel with screen has been estimated by engaging the least square Galerkin's approach executed by the COMSOL MultiPhysics 5.4. The flow was controlled Newtonian and laminar, and the air is forcing fluid that is taken into account. The flow erection has been checked operating the nondimensional Reynolds number with fixed density and viscosity of the air. The resistance coefficient κ of the screen as well refraction coefficient η is fixed. The numerical outcomes are disseminated through the surface plots and graphs for the optimized speed and pressure exerted by the fluid particles. For a particular Reynolds number, it is also perceived via the surface plot; the velocity of the fluid particles after the screen is further increasing in magnitude and behaves not far from the down side of the outlet of the channel. The maximum speed of the particles owns the linear relationship with the Reynolds number and that with the growing in Reynolds number the optimum speed is further optimized. Plus by transferring the angle from 10 to 45 degrees, fluid flow is further accelerated. In addition, the speed of particles and the pressure are also enhancing with the increasing in Reynolds number and retain a parabolic association with it. By transferring the angle from 10° to 45°, the optimum pressure is further reduced at an individual Reynolds number. The drag force applied by the screen is lessening with enhancing the Reynolds number and shifting the angle from 10° to 45°, the resistance to flow is further reduced. We extend the problems finding further and explaining the ratio from local to global Reynolds number on the line passing through the middle of the channel. We found that the local Reynolds number is increasing with the increasing Reynolds number and different for the angles. The ratio from local to global Reynolds number found unique or stable for all the angles of the screen varying in the range from -0.5 to 0.5. Therefore, we expressed the velocity of the particles and the pressure on the line on that nondimensional ratio and concluded that the fluid after passing the screen losses its pressure which results the increase in the velocity of the particles after the screen. Finally, we made the conclusion that the screen can be used as the pressure reducing tool, and it depends upon the angle measuring from the center of the channel in clockwise direction.

Data Availability

No data was required to perform this research.

Conflicts of Interest

The authors declare that there is no conflict of interest regarding the publication of this paper.

Acknowledgments

References

[1] J. W. Elder, "Steady flow through non-uniform gauzes of arbitrary shape," *Journal of Fluid Mechanics*, vol. 5, no. 3, pp. 355–368, 1959.

[2] C. R. C. Santiago, T. Chu, and K. H. Wang, *Study of the Head Loss Associated with a Liquid Owing through a Porous Screen*, 2007.

[3] M. Abid, H. Shaikh, and M. Asif, "Finite element's analysis of fluid flow through the rectangular channel with inclined screens settled at angles," in *2019 2nd International Conference on Computing, Mathematics and Engineering Technologies (ICOMET)*, Sukkur, Pakistan, Pakistan, 2019.

[4] G. A. Sawant, V. M. Mohan, and S. A. Sawant, "Study and analysis of deck inclination angle on efficiency of vibration screen," 2016.

[5] M. Teitel, "Using computational fluid dynamics simulations to determine pressure drops on woven screens," *Bio systems engineering*, vol. 105, no. 2, pp. 172–179, 2010.

[6] G. Hauke and T. J. R. Hughes, "A unified approach to compressible and incompressible flows," *Computer Methods in Applied Mechanics and Engineering*, vol. 113, pp. 385–389, 1993.

[7] A. A. Memon, "Analysis of optimum velocity and pressure of the air flow through the screens with the help of resistance coefficient," *Sukkur IBA Journal of Computing and Mathematical Sciences*, vol. 3, no. 1, pp. 51–57, 2019.

[8] A. A. Memon, H.-u. Shaikh, M. A. Soomro, A. G. Shaikh, and A. H. Shaikh, "Modeling and simulation of newtonian fluid flow through two-dimensional backward-facing step channel with finite element's technique," *Indian Journal of science and technology*, vol. 12, no. 32, pp. 1–6, 2019.

[9] J. Dutta and B. Kundu, "Finite integral transform based solution of second grade fluid flow between two parallel plates," *Journal of Applied and Computational Mechanics*, vol. 5, no. 5, pp. 989–997, 2019.

[10] A. Rauf, "An analytical and semi-analytical study of the oscillating flow of generalized Burgers' fluid through a circular porous medium," *Journal of Applied and Computational Mechanics*, vol. 5, no. 5, pp. 827–839, 2019.

[11] M. Fomicheva, W. H. Müller, E. N. Vilchevskaya, and N. Bessonov, "Funnel flow of a Navier-Stokes-fluid with potential applications to micropolar media," *FactaUniversitatis, Series: Mechanical Engineering*, vol. 17, no. 2, pp. 255–267, 2019.

[12] O. Bazighifan and H. Ramos, "On the asymptotic and oscillatory behavior of the solutions of a class of higher-order differential equations with middle term," *Applied Mathematics Letters*, vol. 107, article 106431, 2020.

[13] O. Bazighifan, "Kamenev and Philos-types oscillation criteria for fourth-order neutral differential equations," *Advances in Difference Equations*, vol. 2020, Article ID 201, 2020.

[14] A. A. Memon, M. A. Memon, K. Bhatti, and G. M. Shaikh, "Finite element simulation of Newtonian and non-Newtonian fluid through the parallel plates affixed with single screen," *European Journal of Pure and Applied Mathematics*, vol. 13, no. 1, pp. 69–83, 2020.

[15] S. Anitha, K. Loganathan, and M. Pichumani, "Approaches for modelling of industrial energy systems: correlation of heat transfer characteristics between magnetohydrodynamics hybrid nanofluids and performance analysis of industrial length-scale heat exchanger," *Journal of Thermal Analysis and Calorimetry*, pp. 1–16, 2020.

[16] K. Loganathan, K. Mohana, M. Mohanraj, P. Sakthivel, and S. Rajan, "Impact of third-grade nanofluid flow across a convective surface in the presence of inclined Lorentz force: an approach to entropy optimization," *Journal of Thermal Analysis and Calorimetry*, 2020.